Spatial contrasts of the Holocene hydroclimate trend between North and East Asia

Yurui Zhang [a, c, *], Hans Renssen [b], Heikki Seppä [c], Paul J. Valdes [d], Jianyong Li [e, f]

[a] Université de Brest- UMR 6523 CNRS / UBO / IRD / Ifremer, LOPS - IUEM - Dumont D'Urville, 29280, Plouzané, France
[b] Department of Natural Sciences and Environmental Health, University of South-Eastern Norway, 3800 Bø i Telemark, Norway
[c] Department of Geosciences and Geography, University of Helsinki, P.O. Box 64, 00014 Helsinki, Finland
[d] School of Geographical Sciences, University of Bristol, Bristol, BS8 1SS, UK
[e] Shaanxi Key Laboratory of Earth Surface System and Environmental Carrying Capacity, College of Urban and Environmental Science, Northwest University, Xi'an 710127, Shaanxi, China
[f] State Key Laboratory of Loess and Quaternary Geology, Institute of Earth Environment, Chinese Academy of Sciences, Xi'an 710061, Shaanxi, China

ARTICLE INFO

ABSTRACT

The hydroclimate over Asia has undergone important changes over the Holocene with spatially asynchronous trends. Proxy-based evidence shows that North Asia was markedly drier than today during the early Holocene, whereas East Asia, influenced by the monsoon system, was substantially wetter. Yet, the causes behind this contrast are only partly understood due to a lack of overview of the most important factors. Here we explore a combination of climate proxies and multiple climate-model simulations to show that the strong contrast between the dry North Asia and wet (mid-latitude) East Asia is explained by a complex interplay between the effects of remnant ice sheets and orbital forcing. In North Asia, the climate was dry due a weakening of the westerlies and reduced atmospheric humidity, linked to the ice sheets in North America and Fennoscandia. In East Asia, contrarily, the orbitally-forced enhancement of the summer monsoons caused the early Holocene climate to be much wetter than during the present-day. These results indicate that the sensitivity of the hydroclimate in Asia to climate-forcings is spatially different, with important implications for the interpretation of past and future climate changes in this region.

© 2019 Elsevier Ltd. All rights reserved.

1. Introduction

Asia covers the highly dynamic monsoon regions at low-latitudes and the vast Siberia at high-latitudes. Driven by the thermal contrast between the Eurasian continent and Pacific Ocean and seasonal variability of solar radiation, winds and precipitation over East Asia monsoon regions are distinctly different between summer and winter, causing the well-known monsoon climate. Summer monsoon precipitation accounts for 80% of the annual rainfall, thus dominating the climate wetness (generally defined as precipitation or moisture condition) and hydrological cycle of region. Through adjustment of the hydrological climate, the temporal and spatial variability of the monsoon circulation influence the livelihood of more than a quarter of the global population. This dynamic summer monsoon in Asia also shows multiple teleconnections to climate changes over other regions (Douville and Royer, 1996). One example is that abrupt climate events of North Atlantic region (Thomas et al., 2007) during the last deglaciation left footprints in monsoon dynamics (Liu et al., 2013). As for high-latitude Asia, its climate history has recently become an important subject because of its huge storage of carbon in peatlands and permafrost that could melt and enhance carbon emissions under current climate warming (Yu et al., 2013). Over the Earth history, climate dynamics over Asia seem to be linked to global climate change at various time-scales, like through teleconnections (Douville and Royer, 1996; Meehl, 1994; Wang et al., 2008b). One of these timescales is the present interglacial, the Holocene (the last 11.5 kyr). With dynamic climate forcings, including orbital-scale solar radiation, melting ice sheets and greenhouse gas (GHG) variations (Berger, 1978; Dyke et al., 2003; Jin et al., 2014; Peltier, 2004; Zhang et al., 2016), the Holocene has gone through different phases of climatic change.

---

* Corresponding author. Université de Brest- UMR 6523 CNRS / UBO / IRD / Ifremer, LOPS - IUEM - Dumont D'Urville, 29280, Plouzané, France.
  E-mail address: yurui.zhang@univ-brest.fr (Y. Zhang).

The Holocene Asian monsoon dynamics have been the subject of numerous proxy-based studies. Several climate proxies, including pollen, chironomids, speleothems, geophysical and geochemical indicators, have been extracted from a variety of archives (such as aeolian sequences, lake sediments, and peat deposits), and have been employed to reconstruct the Holocene climate history over the East Asian monsoon region (Chen et al., 2015, 2008; Li et al., 2017; Zhang et al., 2011). These proxy data can either be quantitatively translated into climate variables (e.g. temperature and precipitation) with the aid of transfer functions derived from systematic observations of the modern day climate (Birks et al., 2012), or they can serve as indicators of hydroclimate, such as lake levels or moisture index (Chen et al., 2008; Zhang et al., 2011). Thanks to the contributions of these proxy records, we have obtained some understanding of the Holocene climate history over this region, although the proxy record sites are scattered and give an incomplete picture. Also, attempts have been made to identify spatially asynchrony patterns of these Holocene climate changes (Chen et al., 2008, 2019; An et al., 2000). By contrast, over high-latitude (northern) Asia the climate history has received only limited attention compared with the well-studied monsoon region, and the mechanisms behind climate changes still remain relatively poorly known. The lack of proxy records from this high-latitude region limits our understanding of detailed spatial climate patterns over the different latitudes of Asia (Sundqvist et al., 2014). Furthermore, mechanism behind the Holocene monsoon climate variability, such as the effects of ice sheets, still remain undiagnosed. A commonly used way to investigate these mechanisms is the direct comparisons of reconstructed time-series of monsoon variability with climate forcings, such as insolation and continental ice volume (Chen et al., 2015; Li et al., 2017). In these Holocene studies, a simplified linear relationship between the size of ice sheets and their climatic effects is assumed, although it is well agreed that the spatial distribution of ice sheets (beside the total amount of ice volume) also influences their climatic impacts (Bromwich et al., 2004; Renssen et al., 2009; Zhang et al., 2016).

With the development of climate modelling, the insolation forcing has been well taken into account in model-simulation studies of the Holocene climate in Asia (Jiang et al., 2012; Jin et al., 2014; Tao et al., 2010). However, the decaying ice sheets (including the Laurentide and Fennoscandian ice sheets) have not yet been explicitly taken into account in these modelling studies. Furthermore, most of numerical studies only employed results of one model, which neglects model-dependent uncertainties, especially given the highly dynamic climate over the monsoon region (An et al., 2000; Jin et al., 2014; Wang et al., 2018). Consequently, a thorough analysis of multi-model simulations performed with full climate forcing is highly demanded to increase the reliability of the simulated Asian climate during the Holocene. With the help of the multi-model simulations, a better understanding of the Holocene can provide a potential analogue for the future climate if there are some similarities between the Holocene and projected future scenario. The temporal-spatial patterns of Holocene climate over mid-latitude Asia have been discussed from different perspectives (An et al., 2000; Chen et al., 2008, 2019; Jin et al., 2014; Zhang et al., 2017). Nevertheless, most of these Holocene studies are based on proxies (An et al., 2000; Chen et al., 2008, 2019), lacking direct proof on mechanisms. Some attempts have been made by combining model and proxydata (Jin et al., 2014; Zhang et al., 2017), but only from 9 ka onward or with a focus on the Holocene thermal maximum, implying that a data-model analysis of the earliest part of the Holocene is still missing.

In the present study, we therefore extend simulations with transient forcings back to the onset of the Holocene to catch the early Holocene transition phase and focus on the general trend of the whole Holocene. The present study investigates the spatial patterns of Holocene wetness over two different latitudinal (North and East) Asian domains and, more importantly, diagnoses drivers behind these spatial patterns by employing simulations of multiple models (LOVECLIM, CCSM3, HadCM3 and FAMOUS). We also specifically identify the effects of ice sheets on the Asian climate by comparing the simulations performed with and without ice sheet forcing. To be more specific, we address tree questions: 1) What are the spatial patterns of Holocene hydroclimate (or wetness) over the Asia domain? 2) What are the drivers (or mechanisms) behind these patterns? 3) How has the melting of ice sheets affected these spatial patterns?

2. Methods

2.1. Simulations

For our model simulations we employed the four climate models LOVECLIM, CCSM3, HadCM3 and FAMOUS. LOVECLIM is a coupled Earth-system climate model. In this study, we applied a version of LOVECLIM that dynamically represents the following components of the climate system: atmosphere, ocean and sea ice, and vegetation. LOVECLIM reproduces reasonably well the main characteristics of the observed surface temperature distribution and right zonal structure of precipitation (Goosse et al., 2010). CCSM3 is a coupled climate model of the ocean–atmosphere–sea-ice–land system; with CAM3 as the atmospheric model, the Parallel Ocean Program (POP) for the ocean, the Community Sea Ice Model (CSIM) for sea ice, and CLM-DGVM for vegetation (Collins et al., 2006). Temperatures and atmospheric circulations in CCSM3 are generally consistent with modern day observations (He, 2011; Jin et al., 2012). The HadCM3 model belongs to the GCM family of models and consists of coupled models for the atmosphere, ocean and sea ice (Gordon et al., 2000; Pope et al., 2000). The model also represents the realistic atmospheric circulation and produces good simulations of precipitation (Pope et al., 2000). FAMOUS is a fast and low-resolution version of HadCM3, and its parameterizations of physical and dynamical processes are almost identical to those of HadCM3 (Smith et al., 2008). More information on these climate models are given in the SI and further comparison among them can be found in Zhang et al. (2018).

With these models, two sets of simulations were employed. The first set of simulations, including the LOVECLIM, CCSM3, HadCM3 and FAMOUS simulations, was performed with full forcing (i.e. solar radiation, atmospheric greenhouse gas (GHG) concentration and decaying ice sheets). The LOVECLIM simulation is an 11.5 kyr long transient run covering the whole Holocene period. Concerned climate forcings in this LOVECLIM simulation are the time-varying orbital-scale insolation (Berger, 1978), GHG (Schilt et al., 2010) and decaying ice sheets. The configuration of the retreating ice sheets, including the Laurentide Ice Sheet and the Fennoscandian Ice Sheet, was prescribed based on radiocarbon datings of geological features (modified from Peltier, 2004), and the associated melt-water release was applied into the oceans. More information on temporal-spatial variability on these forcings and on the setup of this simulation are provided in Zhang et al. (2016). The CCSM3 simulation is the Holocene part of a 21-kyr long simulation performed within the framework of the Trace 21 project (He, 2011). The CCSM3 simulation was forced by transient orbital-scale insolation, GHG, and ice sheets based on the ICE-5G reconstructions and freshwater forcings (He, 2011). The HadCM3 simulation consists of a set of snapshot experiments (the last 30yr average of 300-yr runs) with 1 kyr intervals by considering the GHG, ORB and ice sheet forcings that is comparable with other simulations (Zhang et al., 2018). The FAMOUS simulation was the Holocene part of a

transient simulation covering the last 21 ka, which was forced by the transient GHG and insolation forcings, with prescribed ice sheets and meltwater fluxes into ocean. Therefore, all of these simulations considered the forcings of solar radiation, GHG concentration, and decaying ice sheets (Zhang et al., 2018).

The second set of simulations were conducted with reduced forcing (only with solar radiation and GHG concentration and excluded the ice sheet forcing). This study attempt to disentangle effect of ice sheets by comparing these two sets of simulations. This group of simulations are only available for HadCM3 and LOVECLIM, and termed as HadCM3-OG and LOVECLIM-OG.

2.2. Hydroclimate variables

Total precipitation of the CCSM3, HadCM3 and FAMOUS simulations was analysed in the present study to reflect the wet or dry climate conditions, while the soil moisture data were used for the LOVECLIM simulation as a proxy of wetness. The main reasons for choosing the soil moisture rather than precipitation is that moisture variable is a better indicator for climate wetness in LOVECLIM, because the LOVECLIM model belongs to Earth system Models of Intermediate Complexity (EMIC) and includes a simplified representation for precipitation (with several processes related to precipitation being parameterized), while soil moisture shows water balance and thus wetness of climate (Goosse et al., 2010). Similar spatial patterns between soil moisture and precipitation was detected in LOVECLIM and also in CCSM3 (results not shown). It is worth mentioning that, similar to the LOVECLIM simulation, soil moisture data of CCSM3 can alternatively be used in this analysis, but the data are only available for the annual mean. Since we wanted to analyse summer patterns besides the annual mean, we employed CCSM3's monthly precipitation data in this study. Additionally, soil moisture is closely relevant to biotic proxies (e.g. Anderson and Smith, 1994), permitting realistic comparisons with some proxy-based data.

The precipitation and soil moisture data of all models were normalized into percentage anomalies by reference to the present-day (PI, or 0 ka) climate, in order to avoid the potential uncertainties caused by different units and different ways of presentation of the wetness variable. The normalization procedures included calculating the anomalies of precipitation or moisture from the PI level, and then dividing these anomalies by the value of the present-day, before transferring them into percentage by multiplying by 100. In order to compare different simulations, and also compare them with proxy data, the simulated precipitation and soil moisture are generally termed as "wetness". The Holocene time-series (e.g. Figs. 2 and 5) are shown as the 500-yrs running average in order to obtain overall trends and reduce the noise.

2.3. Proxy records

We collected published proxy-based records on the wet or dry conditions (e.g. precipitation and moisture) of Holocene climate from the East and North Asian domains (20−70°N, 60−125°E). These records are mainly lake sediment data, such as $\delta^{18}O$ and pollen, sediment deposition rate, $CaCO_3$ and magnetic susceptibility. Key information on these records is summarized in Table SI1. It worth pointing out that we did not include cave $\delta^{18}O$ data, because we think that comparison of cave $\delta^{18}O$ data with modelling results deserves a separate study given the complexity of the interpretation of such data and the ongoing debate (e.g. Goldsmith et al., 2017; Liu et al., 2017). These records fall into four groups: individual quantitative reconstructions of total annual precipitation based on pollen data, composite pollen-based aridity index for Eurasian interior, composite moisture reconstructions from central Asia, and

composite moisture index from the Chinese monsoon regions. The composite reconstructions are employed as a whole to illustrate the hydroclimate conditions in a broad region, and we did not further manipulate them, for example by excluding few data from sites that are actually located outside the defined boundaries of our domain (further west), given the composite procedure that has been done by the original studies. Those records data are digitalized by the xyscan tool (http://rhig.physics.yale.edu/~ullrich/software/xyscan/) with a minimum of 3 points per thousand years for records with low-frequent variability (smooth time-series curve), and with a maximum of 13 points per thousand years for high-frequency variability (saw-tooth time-series curve). Thus, the accuracy in the digitalization is acceptable for representing the general trends, although uncertainties in exact values are unavoidable.

In order to compare with simulated wetness patterns, the individual quantitative records have been divided into two groups for northern and southern regions with a boundary of 40°N as marked in Fig. 1. The records in the same regions have been further compiled into one reconstruction to represent North or East Asia. This compilation includes two steps: 1) binning data points of each individual record with 0.5 kyr intervals, and taking the median (of all these points) to represent a given bin; 2) taking an average of all records for each bin to represent the final regional reconstruction. There are 10 quantitative precipitation records in the entire domain, with 4 records belonging to the North Asia group and the rest (6 records) belonging to the East Asia group. For composite reconstruction, pollen-based aridity index (equivalent to reversed moisture index) has been conducted by Zhang and Feng (2018), based 19 pollen sequences. As for large scale moisture index for arid central Asia (falls into our North Asia), the reconstruction has been done by Chen et al. (2008), and is composed of 11 various records from lake sediments. The moisture index has been compiled from 10 $\delta^{18}O$ records of lake sediment over the southern China by Zhang et al. (2011).

3. Results

We first analyse wetness in the multiple simulations with focus on North and East Asian domains, as marked in Fig. 1. These model results will be accordingly compared with proxy-base data, before briefly analysing the effect of ice sheets.

3.1. Spatially heterogeneous wetness patterns over mid- and high-latitude Asia

3.1.1. Simulated wetness anomalies at 11.5 ka

Compared with the present-day (0 ka), the overall spatial patterns of wetness at the onset of Holocene (11.5 ka) signify a striking north-south (N−S hereafter) contrast. The negative anomalies in North Asia represent a drier than the present-day climate, in contrast with positive anomalies found over East Asia (Fig. 1 & Fig. S1). The magnitudes of those anomalies (in ensemble average) range from −40% (relatively dry) to 50% (wetter) in our studied domain, with the bigger anomalies in summer (JJA) than in annual mean (ANN). Although there are some regional variations, the positive anomalies overall cover the East Asia with a boundary 35−40°N. In the studied domain, the maximum positive values, up to ~50%, have been found over East Asia with a smaller magnitude in ANN than in JJA. The negative anomalies in North Asia spread between −30% and −40%, with maximum values reached over the central continent. Further inspection reveals that the positive values of ensemble-mean wetness for JJA along the Siberian coast are mainly derived from the FAMOUS simulation. This is probably because of the less early Holocene sea ice coverage than at 0 ka in the East Siberian Sea that allow an active hydrological cycle (Fig. 7a
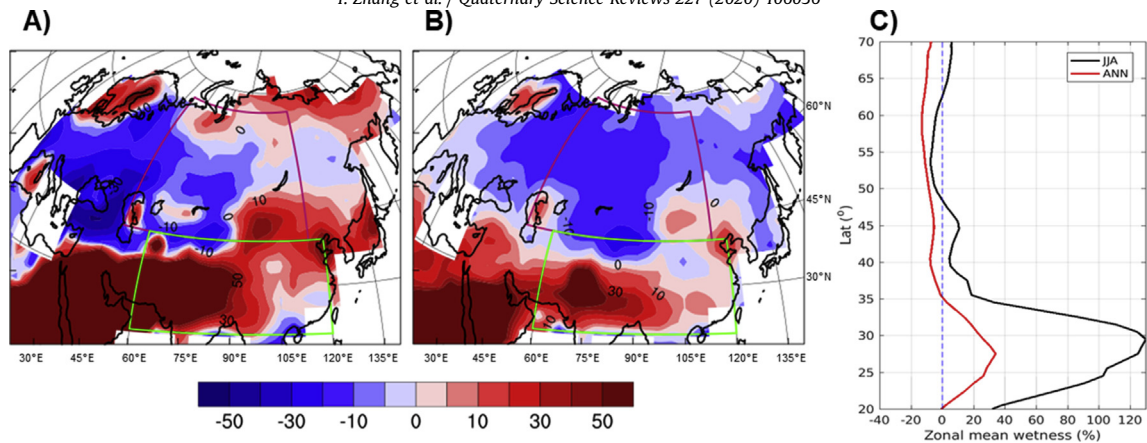
Fig. 1. Spatial pattern of simulated precipitation anomalies at 11.5 ka. (A) and (B) shown ensemble mean for JJA and ANN, as a standardized anomaly (in %) from the PI. (C) Zonal-averaged wetness anomalies for the region 55−115°E, 10−70°N. LOVECLIM data are not included in the ensemble mean and are separately provided in SI.

of Zhang et al., 2018). The zonal mean wetness anomalies (for the 55−115°E) also show this N−S wetness contrast (Fig. 1C), with a distinct enhancement in the south and slightly negative anomalies in the north. Also, the simulated moisture in LOVECLIM, which is not included in the ensemble-mean precipitation, reveals a similar N−S contrast with 30% anomalies in the south and 40% less wet in the north, as shown in Fig. SI1.

3.1.2. Holocene wetness trend in transient simulations across North and East Asia

Given this spatial contrast, the standardized wetness trends over the Holocene were investigated in terms of the North (50−115°E, 40−70°N) and East Asia (60−120°E, 20−40°N) regions respectively. The 5° westward shift of the North Asia domain roughly represents a slight northwestward tilt in order to exclude
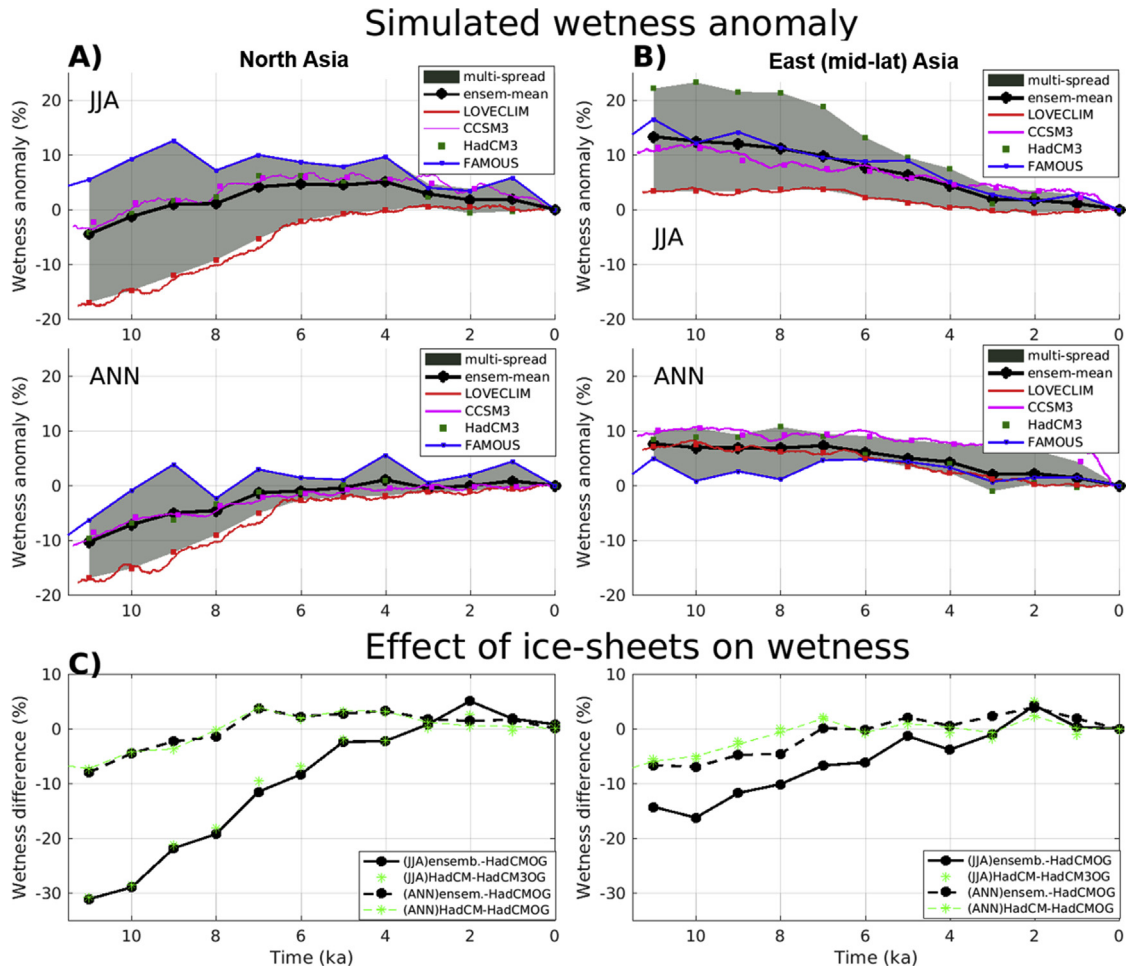

Fig. 2. Simulated Holocene wetness (precipitation or soil moisture) trend over North Asia (50−115°E, 40−70°N) and East Asia (60−120°E, 20−40°N), shown as anomaly from 0 ka in the upper two panels (A & B). The last panel (C) illustrates the effect of ice-sheet on wetness shown as the wetness difference between the simulation with and without ice sheets. The black (green) color indicates the wetness differences between the ensemable mean (HadCM3) and the HadCMOG simulation, with dashed-dots line for summer (JJA) and solid line for annual mean (ANN). (For interpretation of the references to color in this figure legend, the reader is referred to the Web version of this article.)

the coastal region in the east, which was actually influenced by ocean. This boundary is a bit more to the north than the traditional boundary between South and North China, which is usually defined by the Qinling Mountains (~34°N). However, our study is dealing with large geographical domain in Asia rather than only focusing on the Chinese monsoon region. Actually, with our division, the East Asian domain covers the whole Chinese monsoon region and transitional regions of monsoon climate. These transitional regions are only influenced by the monsoon circulation when the monsoon is strong and is accompanied by northward extension of monsoon flows (otherwise, they are outside the influences of the monsoon). In addition, we conducted a sensitivity test on slightly different selected regions (e.g. boundary at 35°N) and the results still show similar N−S contrasts. It is worth pointing out that we attempted to divide Asia into two sub-regions (on different scales) based on their common features (e.g. hydroclimate trend here) in order to explain this feature by exploring the underlying processes, rather than consider the sub-region as a homogeneous region.

In the North Asian domain, the simulations show an overall lower moisture or precipitation in the early to mid-Holocene relative to the present-day, with an increasing wetness over the course of the Holocene (Fig. 2A). At the onset of the Holocene, the ensemble-mean wetness anomalies show a ~10% reduction in the annual mean, varying from ~18% in LOVECLIM to ~8% in FAMOUS. Subsequently, simulated wetness increased by 10−20% over the course of the Holocene. Summer wetness shows smaller changes (with the ensemble mean of ~5% enhancement over the course of the Holocene), ranging from ~18% enhancement in LOVECLIM and to ~5% enhancement in CCSM3 and HadCM3, and to even a small reduction (+5%) in FAMOUS. Noticeably, the ensemble mean of wetness for JJA shows an increasing trend from −5% to +5% by 6 ka, after which it decreases toward to 0 ka.

In contrast to the North Asian domain, the simulations suggest a higher Holocene wetness in East Asia than at present-day, with decreasing wetness (precipitation or moisture) trend over the course of the Holocene (Fig. 2B). The ensemble mean shows 8% wetter (with ±2% inter-model spreads) annual conditions at the onset of the Holocene, and decrease over time till 0 ka. The wetness anomalies in summer are above 10%, which is stronger than in the annual mean results. The inter-model range is also large in summer, spreading from less than 5% in LOVECLIM to over 20% in FAMOUS simulations. These positive wetness anomalies gradually decrease over the course of the Holocene. Therefore, the most distinct feature is the N−S contrast in wetness anomalies during the Holocene: reduced wetness in the North Asia contrasts with enhanced wetness in the East-Asia at the onset of the Holocene; and opposite Holocene trends between the North Asia (increasing) and the East Asian monsoon region (decreasing).

3.2. Proxy-based Holocene wetness reconstructions

At the onset of the Holocene, the proxy-based wetness reconstructions also reveal a reduction of precipitation and moisture in North Asia compared to 0 ka and positive wetness anomalies in East Asia (Fig. 3). This agrees with the simulated N−S contrast in wetness anomalies. The quantitative reconstruction for North Asia (compiled from 4 individual records) shows ~30% drier conditions in the early Holocene from the onset of the Holocene until 8 ka than 0 ka (Fig. 3A). This drier early Holocene condition is well consistent with two other composited proxy-based reconstructions. One is pollen-based aridity index reconstruction compiled from 19 individual pollen records Zhang and Feng (2018), which shows more than one unit drier (out of 3 units) conditions at the onset of the Holocene. Another is moisture reconstruction for central Asia region compiled from lake level data by Chen et al. (2008), suggesting

two units less (out of 3 units) moisture during the early Holocene. By contrast, for East Asia the proxy-based reconstructions of precipitation and moisture agree with simulated results on the sign of wetness anomalies at 11.5 ka (Figs. 2 and 3B). The quantitative reconstruction (compiled from 6 individual records) suggests 20% more precipitation during the early Holocene than 0 ka. The composite moisture index derived from geochemical proxies (Zhang et al., 2011) also indicates enhanced moisture with even a larger magnitude than in the quantitative reconstruction. Overall, these multiple lines of proxy data show that at the onset of Holocene East Asia was drier, contrasting with wetter condition over South Asia.

Over the course of the Holocene, the proxy-based moisture and precipitation reconstructions reveal an increasing Holocene trend over North Asia but a decreasing trend in mid-latitudinal East Asia (Fig. 3), which agrees with the simulated wetness trend. For North Asia, the simulations and most of proxy data show an increasing Holocene wetness trend (toward 0 ka), although the specific magnitudes and their agreement (between the proxy-based reconstructions and the simulated Holocene wetness) vary over time (Figs. 2 and 3a). During the early Holocene (before 8 ka), the quantitative precipitation reconstruction, pollen-based aridity index and the reconstructed moisture scale suggest 20−30% drier condition than at 0 ka, which is in the range of simulated wetness anomalies, despite the larger magnitude than ensemble mean of multi-simulations. From 8 ka to 5−4 ka, the quantitative precipitation reconstruction and moisture data suggests a wetter climate than at 0 ka. This feature is weak in the simulations and absent in pollen-based aridity index reconstruction. From ~3 ka onward, both data and simulated wetness data indicate minor changes toward 0 ka. Overall, simulations and proxy data agree well in terms of the sign of climate wetness at onset of the Holocene and of general Holocene trend of wetness.

For East Asia, proxy-based reconstructions of precipitation and moisture agree with simulated results, which show the decreasing Holocene wetness trend (Figs. 2 and 3B). During the early Holocene, proxy datasets show a positive wetness range from 20% to 40% anomalies from 0 ka, although the trends in those two sets data are slightly different. From 6 ka onward, two sets of proxy data show a 40% decrease toward 0 ka, which is stronger than simulated decrease (~10%). In summary, the proxy data support this simulated north-south (N-S) contrast pattern of Holocene wetness trend.

3.3. Effect of the ice sheets on early-Holocene wetness

Two additional simulations (HadCM3-OG and LOVECLIM-OG), only forced with orbital-scale radiation and GHG, allow us to disentangle the effect of ice sheets on Asian wetness during the early Holocene. As shown in Fig. 2C, the wetness differences between the simulations with and without ice sheets are negative during the early Holocene, indicating the drying effect of the ice sheets. This drying effect is much larger in North -Asia than in the East Asian region. In summer, these differences are up to 30% in the north compared with 8% in the East Asia. In annual mean, although the magnitude of this drying effect is small, North Asia is still influenced more by the ice sheets (~10%) than the over East Asian region (only ~7%). In addition, the differences between the ensemble mean wetness of full-forcing simulations and HadCM3-OG simulation further confirm that the drying effect of ice sheets over North Asia are much larger than over East Asia. The 850 hPa wind differences between the simulation with and without ice sheets are rather small and show no clear spatial pattern.

4. Discussion

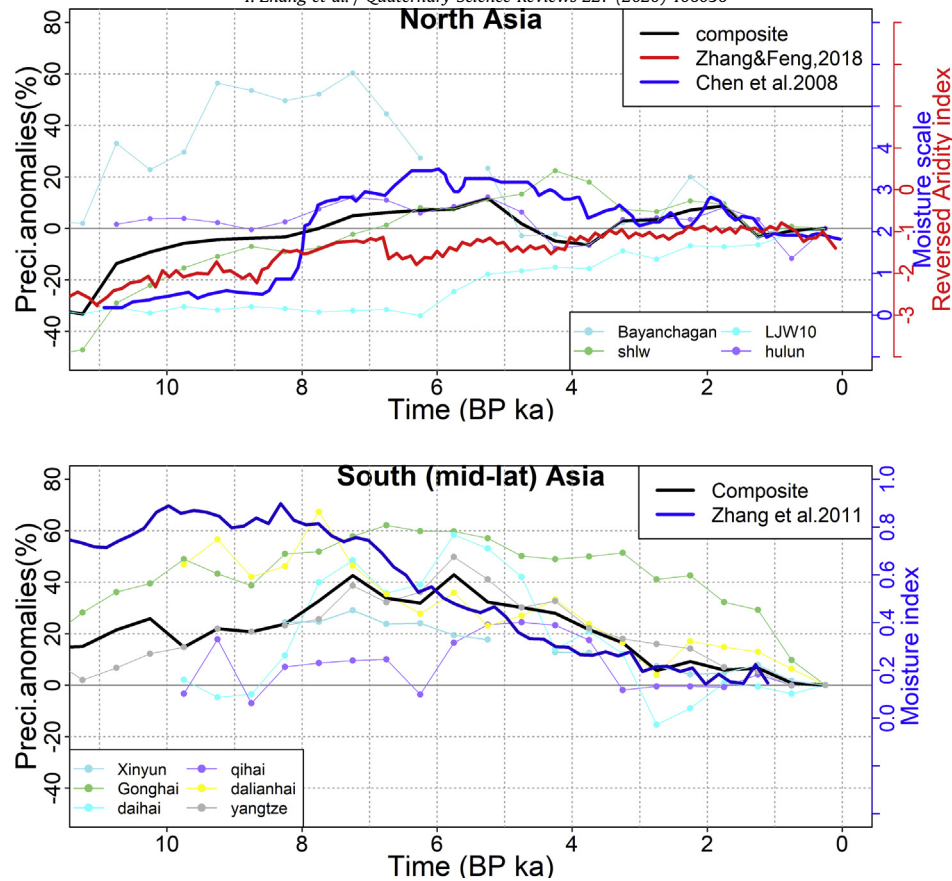The drivers of the N−S contrast of Holocene wetness can be

Fig. 3. Proxy-based wetness trends during the Holocene in North Asia (**A**) and in East Asia (**B**). Black thick lines are combined (quantitative) precipitation records, with dot-line indicating the original data in background. The blue lines in two plots are moisture index reconstructions, derived from Chen et al. (2008) and Zhang et al. (2011) presenting the North Asia and East Asia. The red line for North Asia is the reversed aridity index reconstruction (based on pollen) derived from Zhang and Feng (2018). Locations of these records are given in Table SI. (For interpretation of the references to color in this figure legend, the reader is referred to the Web version of this article.)

explained by a complex interplay between the effects of remnant ice sheets and orbital forcing, as revealed by the below analysis on thermodynamic processes.

4.1. Mechanisms behind wetness changes over North Asia

4.1.1. Weakening of westerlies during the early Holocene

Climate conditions, like wetness, of given regions are closely linked to atmospheric circulations. For North Asia, atmospheric circulation is dominated by the zonal wind over the mid-high latitudes, known as the westerlies. The following analysis will only focus on zonal wind strength changes. On larger scale (NH), the striking feature of the zonal wind during the early Holocene (with good inter-model agreements) is enhanced strength of the zonal wind over the down-wind region of the Laurentide Ice Sheet (Fig. SI2). We further zoom into the domain of Asia to have a closer look at the change in westerlies. In order to quantify westerly differences in the domain of Asia, the zonal wind at 850 hPa level (JJA) at 11.5 ka was standardized to anomalies (in %, refer to 0 ka) and their zonally-averaged results were plotted along latitudes (Fig. 4A). At 11.5 ka, these zonal-mean results of all simulations show overall reduced westerlies over north of 40°N with a magnitude of ~50%. These reduced westerlies at the onset of the Holocene brought less moisture from the oceanic sources area in the west, and thus contributed to the relatively dry conditions over North Asia. By contrast, the region south of 40°N displays an overall enhanced zonal wind at 11.5 ka, although the wetness over this region is dominated by monsoon-related circulation. The enhanced

850 hPa can be the result of a southward shift of the jet-stream, or a strengthening of zonal winds (related to enhanced monsoon circulations).

This switch at the latitude of ~40°N also agrees well with the proxy-based wetness data at 11.5 ka (Fig. 4B). The strong negative early Holocene anomalies, up to 40–80%, have been found over North Asia (north of 40°N) (except one point of Sihailongwan that belongs to northern but shows a near-zero positive anomaly). For the region south of 40°N, the positive wetness anomalies for all records were within 60%. Thus, the reduced early Holocene wetness over North Asia and related decreasing trend can be partly explained by reduced westerlies.

4.1.2. Reduced early Holocene humidity due to existence of the ice sheets

The presence of the ice sheets during the early Holocene substantially reduced air humidity over North Asia. As represented by the differences of atmospheric humidity between the HadCM3 (full) and HadCM3OG shown in Fig. 4C, this reduction was up to 10% at 11.5 ka and its magnitude decreased over time till the ice sheets finally melted out at around 7 ka. The presence of ice sheets over the up-wind region makes the air drier than in ice-free surface condition and this drying effect can be further conveyed to the downstream region. For instance, ice cover can reduce or prevent sources of evaporation, thus decreasing the water vapor supply to the air that is being transported eastward by the atmospheric circulation. Meanwhile, the ice sheets contribute to cooling of the air that can contain less moisture relative to warm air. Additionally, we
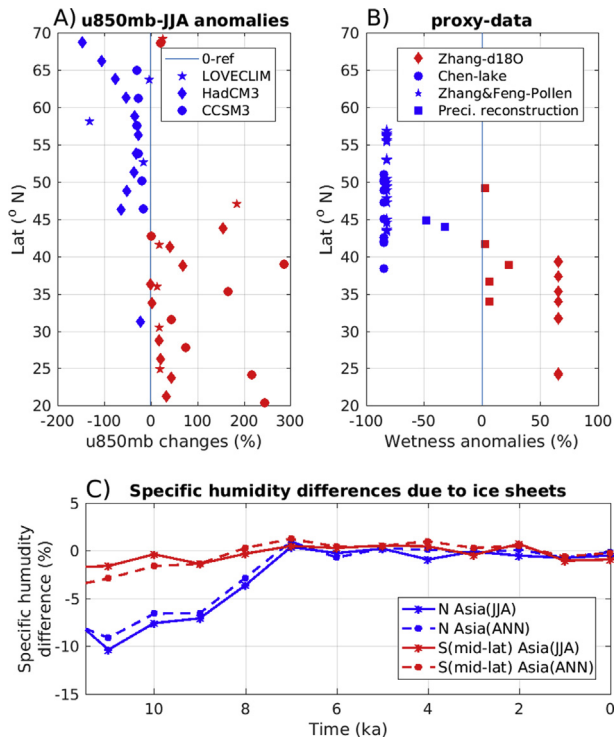
Fig. 4. Zonally-averaged summer (JJA) zonal wind anomalies (westerlies, at 850 hPa) at 11.5 ka (in % ref to PI) change over latitudes (A). Proxy-based wetness anomalies (in %) shown along the latitudinal transect (B). Specific humidity differences between the simulation with and without ice sheet that explained the drying effect of ice sheets (C).

investigated the difference in westerlies between the simulations with and without ice sheets, and only found small differences. The small magnitude of these differences suggests a secondary role of ice sheets on the strength of the atmospheric circulation. The drier effect of the ice sheets in the North Asian domain, as found above, is mainly due to reduced air humidity when the ice sheets were present. Therefore, we conclude that reduced air humidity together with reduced westerlies strength led to the drier early-Holocene climate than present in North Asia. As for the East Asia domain, the differences in air humidity between the simulations with and without ice sheets are much smaller than in North Asia. Therefore, the drying effect of ice sheets over the East Asia domain is relatively small.

4.2. Monsoon circulation mainly responsible for wetness change over East Asia

For the southern East Asia region, the differences of westerly winds and humidity between 11.5 ka and 0 ka are small, and the reducing wetness trend over the course of the Holocene can actually be explained by decreasing monsoon strength. In order to measure monsoon strength, the monsoon index was calculated from wind fields at 850 hPa with the methods given by Wang and Fan (1999). This calculation follows the suggestion given by Wang et al. (2008a,b), in which they compare a series of monsoon indices and recommend the one that provides the best correlation to monsoon variability. The calculated monsoon index (based on HadCM3, CCSM3 & LOVECLIM results) at the onset of Holocene was stronger than the present-day, with 30% enhancement in CCSM3 and 65% in HadCM3 (Fig. 5). Over the course of the Holocene, the monsoon index illustrates a decreasing trend in monsoon strength. Consequently, the decreasing Holocene wetness trend can be
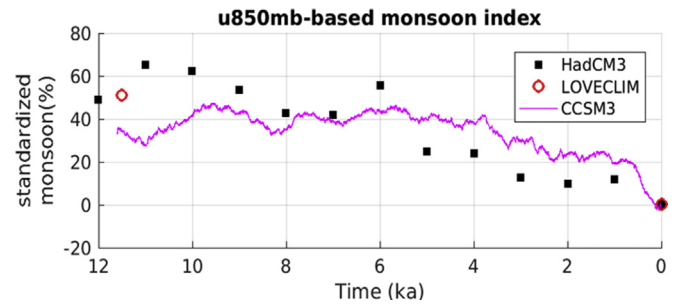
Fig. 5. Monsoon index changes (in %) during the Holocene. These results are calculated from zonal wind fields at 850 hPa, using a method of Wang and Fan (1999) and Wang et al. (2008a,b).

explained by a weakening of the monsoon, given the precipitation amount is tightly linked to the monsoon strength over this region and the monsoon was greatly enhanced (by 30−50%) during the early Holocene. The contribution of both westerlies and their interactions with the enhanced monsoon circulations to wetness changes probably is relatively small. The interactions are the results of sets of processes, and there should be a balance among them for a given climatic context. For the studied Asian region, westerlies (in the North) and monsoon circulation (in the South) compete for space over the transition region, and this change in circulation itself can induce a further chain of changes. For instance, this strong monsoon circulation during the early Holocene could restrict the spatial influence of the mid-latitude westerly wind and enhance the meridional temperature gradient over a given region that favors to enhanced westerlies locally. Nevertheless, it is difficult to clearly separate these interactions, unless the sources of precipitation (water vapor) can be tracked down from the south (Pacific) or the west (Eurasia, or further west to N Atlantic) by adding tracers to the atmospheric circulations in a model, which however, is beyond the scope of the present study. In addition, as a direct driver of Asian monsoon circulations, thermal contrasts between the Asian Continent and Pacific Ocean also show an overall decreasing trend over the course of the Holocene (Fig. SI3). The thermal contrast refers to temperature differences between the continental and oceanic regions. Those regions are chosen by referring to Zhao et al. (2007) and Xiao et al. (2016), who found that relative changes over those two regions probably represent changes in monsoon circulation intensity, as they roughly correspond to the Mongolian low and the West Pacific subtropical high.

In order to track down the sources of this strong early Holocene monsoon circulation, we have further considered how the monsoon index is calculated. By definition, the monsoon index reflects relative changes of two regions. Further investigations of those two individual regions reveal that changes of zonal winds over the region near the Equator (the western near-equatorial Pacific Ocean) is larger than the change in the region over mid-latitudes (Fig. SI4). This implies that the large values for monsoon index during the early Holocene are mainly due to changes in the equatorial Pacific Ocean, and the Holocene monsoon strength changes and wetness changes in East Asia are thus primarily dominated by processes occurring at low latitudes. One possible explanation for this strong Early-Holocene monsoon circulation could be related to variability of Intertropical Convergence Zone (ITCZ). It has been suggested that the orbital forcing produces an expansion/contraction of ITCZ and the presence of the ice sheets in mid-to high-latitude can shift it meridionally (Singarayer et al., 2017). For instance, Broccoli et al. (2006) found a southward shift during the Last Glacial Maximum (LGM) when ice sheets partially covered North America and Eurasia and with the similar orbital

forcing than PI. For the early Holocene, the net effects of these two factors cause an overall northward position of the ITCZ compared to PI (Sachs et al., 2018), which is consistent with the reduced zonal wind over the nearby Equatorial Pacific Ocean, as shown in Fig. SI4. This explanation is consistent with Beck et al. (2018), who further emphasized the importance of interhemispheric insolation gradients on the East Asian Summer Monsoon intensity.

4.3. Comparisons with previous studies

The relative importance of ice sheet and the orbital-scale solar radiation over the glacial-and interglacial cycle has been extensively discussed. For instance, it has been suggested that the presence of ice sheets during MIS-13 (Marine Isotope Stage, at 524–474 ka) reinforced the Asian monsoon via interactions between the ocean and atmosphere, for example through the stationary waves (Yin et al., 2008, 2009; Sundaram et al., 2012). The first response would be that our results (with no clear effect for the early-Holocene monsoon) are at odds with these findings. However, a closer investigation reveals that the different early-Holocene response compared to MIS-13 is explainable, because the forcings are not identical for these two periods and the climate system might behave differently during the early Holocene and MIS-13. The early Holocene is under the process of transition from the last glacial maximum to present day climate, with ice sheet melting and associated freshwater release into ocean, while there was no freshwater forcing in these MIS-13 studies. More importantly, the locations of the Eurasian ice sheets are quite different between the Holocene setup (Zhang et al., 2016) and MIS-13 setup (Yin et al., 2008). For instance, according to the ice sheet reconstructions, our Eurasian ice sheet is mainly located in Fennoscandia during the early Holocene, while the MIS-13 Eurasian ice sheet is centered at north Eurasia (Yin et al., 2008), which is much more to the East than in our case. Meanwhile, the orbital configuration between the MIS-13 and the early Holocene are not exactly the same—with similar precession but different eccentricity and obliquity. Therefore, it is not surprising to see some differences in the relative importance of ice sheets and orbital forcings between MIS-13 and the Holocene. Accordingly, a systematical comparison of these different geological epochs would be interesting and deserves a separate study.

Compared to previous studies on spatial patterns of Holocene climate over Asia, the innovation of the present study is that we employed multiple-model transient simulations to sketch the overall wetness trend over the whole Holocene for the first time. This multi-model simulation analysis provides a consistent mechanism for previous proxy-based Holocene climate history (An et al., 2000; Chen et al., 2008, 2019) and fills the gap of the missed early-Holocene transition phase (Jin et al., 2014; Zhang et al., 2017), and also highlights the Holocene hydroclimate trend over high-latitude Asia. The effect of ice sheets has been specifically diagnosed in the present study. Our results on the relative influence of the orbital forcing and ice sheet are compatible with a previous study on the relative importance these two factors on the Holocene climate (Jin et al., 2012), although the scale of ice sheets is different. Jin et al. (2012) investigated the effects of these two forcings at 8.5 ka in an equilibrium experiment and found that the ice sheets had a substantial cooling effect and drying influence over high latitudes, while the contribution of the ice sheets was small to climate changes in central Asia during the early Holocene. Our multi-model simulations go further back to the onset of the Holocene (11.5 ka) with the large scale Laurentide Ice Sheet and the remains of Fenoscandian Ice Sheet, during which more intensive or southward extended effects can be expected. At the onset of the Holocene, we find a clear drying effect of ice sheets over a broad northern region (up to 70N), which actually covers the high-latitude region and a part of Central Asia as employed by Jin et al. (2012). This is due to the more extensive ice sheet at 11.5 ka than at 8.5 ka.

These similarities and differences between our results and previous studies actually reflect that there are a variety of ways to divide climatic domains due to the regional differences of climate at various levels. This division can also change with time periods of interest. For instance, at the onset of the Holocene, the presence of the large scale ice sheets exerts a more southward extended effect than at 8.5 ka as found by Jin et al. (2012), which makes part of mid-latitude Asia of Jin et al. (2012) fall into our North Asia region. In addition, a different focus can modify this division. For instance, Chen et al. (2008, 2019) and Jin et al. (2012) define the monsoon regions and central Asia based on proxy record studies with special interests on the early Holocene aridity over the central Asia. In the present study, we are interested in N–S spatial contrast between the North and East Asia and underlying mechanisms. Furthermore, we intended to extend our northern domain further northward to shed some light on high-latitude Asia, like Siberia, where proxy-based records are sparse (Sundqvist et al., 2014). This makes our domain larger than in the proxy-based studies of Chen et al. (2008, 2019).

5. Conclusions

Our analysis clearly indicated that the Holocene hydroclimate trends are not the same everywhere in Asia. Multiple simulations signify the spatial contrast of the Holocene wetness evolution between North and East Asia. Over North Asia, wetness shows an increasing Holocene trend with a drier early Holocene, while the East Asia region has a decreasing wetness trend over the Holocene. This N–S contrast in the Holocene wetness trend is supported by proxy-based evidences, including quantitative precipitations records and composite moisture reconstructions.

This N–S contrast can be attributed to different dominant mechanisms between North and East Asia. The relatively low early Holocene wetness over North Asia is caused by weakening of westerly winds and reduced air humidity linked to the presence of ice sheets. By contrast, in East Asia the enhanced wetness at 11.5 ka and the following decreasing Holocene trend is caused by the strong monsoon circulation at onset of the early Holocene and its subsequent weakening, as responses to the orbitally-induced insolation thermal dynamics. We find a wetter hydroclimate in the East Asian region during the early Holocene similar to the predicted higher rainfall for future, as suggested by the CMIP5 simulations under the RCP8.5 scenario (Li et al., 2015). This implies that the early Holocene can have important implications for interpreting the future hydroclimate over the East Asia region.

Appendix A. Supplementary data

Supplementary data to this article can be found online at https://doi.org/10.1016/j.quascirev.2019.106036.

References

An, Z., Porter, S.C., Kutzbach, J.E., Xihao, W., Suming, W., Xiaodong, L., Xiaoqiang, L., Weijian, Z., 2000. Asynchronous Holocene optimum of the east Asian monsoon. Quat. Sci. Rev. 20.

Anderson, R.S., Smith, S.J., 1994. Paleoclimatic interpretations of meadow sediment and pollen stratigraphies from California. Geology 22, 723–726. https://doi.org/10.1130/0091-7613(1994)022<0723:PIOMSA>2.3.CO;2.

Beck, J.W., Zhou, W., Li, C., Wu, Z., White, L., Xian, F., Kong, X., An, Z., 2018. A 550,000-year record of East Asian monsoon rainfall from [10]Be in loess. Science 360, 877–881. https://doi.org/10.1126/science.aam5825.

Berger, A.L., 1978. Long-term variations of caloric insolation resulting from the earth's orbital elements. Quat. Res. 9, 139–167. https://doi.org/10.1016/0033-5894(78)90064-9.

Birks, H.J.B., Lotter, A.F., Juggins, S., Smol, J.P. (Eds.), 2012. Tracking Environmental Change Using Lake Sediments, Developments in Paleoenvironmental Research. Springer Netherlands, Dordrecht.

Broccoli, A.J., Dahl, K.A., Stouffer, R.J., 2006. Response of the ITCZ to northern hemisphere cooling. Geophys. Res. Lett. 33, L01702. https://doi.org/10.1029/2005GL024546.

Bromwich, D.H., Toracinta, E.R., Wei, H., Oglesby, R.J., Fastook, J.L., Hughes, T.J., 2004. Polar MM5 simulations of the winter climate of the Laurentide ice sheet at the LGM. J. Clim. 17, 3415–3433. https://doi.org/10.1175/1520-0442(2004)017%3c3415:PMSOTW%3e2.0.CO;2.

Chen, F., Chen, J., Huang, W., Chen, S., Huang, X., Jin, L., Jia, J., Zhang, X., An, C., Zhang, J., Zhao, Y., Yu, Z., Zhang, R., Liu, J., Zhou, A., Feng, S., 2019. Westerlies Asia and monsoonal Asia: spatiotemporal differences in climate change and possible mechanisms on decadal to sub-orbital timescales. Earth Sci. Rev. 192, 337–354. https://doi.org/10.1016/j.earscirev.2019.03.005.

Chen, F., Xu, Q., Chen, J., Birks, H.J.B., Liu, J., Zhang, S., Jin, L., An, C., Telford, R.J., Cao, X., Wang, Z., Zhang, X., Selvaraj, K., Lu, H., Li, Y., Zheng, Z., Wang, H., Zhou, A., Dong, G., Zhang, J., Huang, X., Bloemendal, J., Rao, Z., 2015. East Asian summer monsoon precipitation variability since the last deglaciation. Sci. Rep. 5 https://doi.org/10.1038/srep11186.

Chen, F., Yu, Z., Yang, M., Ito, E., Wang, S., Madsen, D.B., Huang, X., Zhao, Y., Sato, T., John, B., Birks, H., Boomer, I., Chen, J., An, C., Wünnemann, B., 2008. Holocene moisture evolution in arid central Asia and its out-of-phase relationship with Asian monsoon history. Quat. Sci. 27, 351–364. https://doi.org/10.1016/j.quascirev.2007.10.017.

Collins, W.D., Bitz, C.M., Blackmon, M.L., Bonan, G.B., Bretherton, C.S., Carton, J.A., Chang, P., Doney, S.C., Hack, J.J., Henderson, T.B., Kiehl, J.T., Large, W.G., McKenna, D.S., Santer, B.D., Smith, R.D., 2006. The community climate system model version 3 (CCSM3). J. Clim. 19, 2122–2143. https://doi.org/10.1175/JCLI3761.1.

Douville, H., Royer, J.-F., 1996. Sensitivity of the Asian summer monsoon to an anomalous Eurasian snow cover within the Météo-France GCM. Clim. Dyn. 12, 449–466. https://doi.org/10.1007/BF02346818.

Dyke, A.S., Moore, A., Robertson, L., 2003. Deglaciation of North America (No. 1574).

Goosse, H., Brovkin, V., Fichefet, T., Haarsma, R., Huybrechts, P., Jongma, J., Mouchet, A., Selten, F., Barriat, P.-Y., Campin, J.-M., Deleersnijder, E., Driesschaert, E., Goelzer, H., Janssens, I., Loutre, M.-F., Morales Maqueda, M.A., Opsteegh, T., Mathieu, P.-P., Munhoven, G., Pettersson, E.J., Renssen, H., Roche, D.M., Schaeffer, M., Tartinville, B., Timmermann, A., Weber, S.L., 2010. Description of the Earth system model of intermediate complexity LOVECLIM version 1.2. Geosci. Model Dev. (GMD) 3, 603–633. https://doi.org/10.5194/gmd-3-603-2010.

Goldsmith, Y., Broecker, W.S., Xu, H., Polissar, P.J., deMenocal, P.B., Porat, N., Lan, J., Cheng, P., Zhou, W., An, Z., 2017. Northward extent of East Asian monsoon covaries with intensity on orbital and millennial timescales. Proc. Natl. Acad. Sci. U.S.A. 114, 1817–1821. https://doi.org/10.1073/pnas.1616708114.

Gordon, C., Gregory, J.M., Wood, R.A., 2000. The simulation of SST, sea ice extents and ocean heat transports in a version of the Hadley Centre coupled model without flux adjustments, 16, 147–168.

He, F., 2011. Simulating Transient Climate Evolution of the Last Deglaciation with CCSM3. University of Wisconsin-Madison, Madison, WI.

Jiang, D., Lang, X., Tian, Z., Wang, T., 2012. Considerable model–data mismatch in temperature over China during the mid-holocene: results of PMIP simulations. J. Clim. 25, 4135–4153. https://doi.org/10.1175/JCLI-D-11-00231.1.

Jin, L., Chen, F., Morrill, C., Otto-Bliesner, B.L., Rosenbloom, N., 2012. Causes of early Holocene desertification in arid central Asia. Clim. Dyn. 38, 1577–1591. https://doi.org/10.1007/s00382-011-1086-1.

Jin, L., Schneider, B., Park, W., Latif, M., Khon, V., Zhang, X., 2014. The spatial–temporal patterns of Asian summer monsoon precipitation in response to Holocene insolation change: a model-data synthesis. Quat. Sci. Rev. 85, 47–62. https://doi.org/10.1016/j.quascirev.2013.11.004.

Li, J., Dodson, J., Yan, H., Cheng, B., Zhang, X., Xu, Q., Ni, J., Lu, F., 2017. Quantitative precipitation estimates for the northeastern Qinghai-Tibetan Plateau over the last 18,000 years. J. Geophys. Res. Atmosphere 122, 5132–5143. https://doi.org/10.1002/2016JD026333.

Li, X., Ting, M., Li, C., Henderson, N., 2015. Mechanisms of Asian summer monsoon changes in response to Anthropogenic forcing in CMIP5 models*. J. Clim. 28, 4107–4125. https://doi.org/10.1175/JCLI-D-14-00559.1.

Liu, J., Chen, S., Chen, J., Zhang, Z., Chen, F., 2017. Chinese cave δ^{18}O records do not represent northern East Asian summer monsoon rainfall. Proc. Natl. Acad. Sci. U.S.A. 114, E2987–E2988. https://doi.org/10.1073/pnas.1703471114.

Liu, Y.H., Henderson, G.M., Hu, C.Y., Mason, A.J., Charnley, N., Johnson, K.R., Xie, S.C., 2013. Links between the east Asian monsoon and North Atlantic climate during the 8,200 year event. Nat. Geosci. 6, 117–120. https://doi.org/10.1038/ngeo1708.

Meehl, G.A., 1994. Influence of the land surface in the Asian summer monsoon: external conditions versus internal feedbacks. J. Clim. 7, 1033–1049. https://doi.org/10.1175/1520-0442(1994)007<1033:IOTLSI>2.0.CO;2.

Peltier, W.R., 2004. Global glacial isostasy and the surface of the ice-age earth: the ice-5G (VM2) model and grace. Annu. Rev. Earth Planet Sci. 32, 111–149. https://doi.org/10.1146/annurev.earth.32.082503.144359.

Pope, V.D., Gallani, M.L., Rowntree, P.R., Stratton, R.A., 2000. The impact of new physical parametrizations in the Hadley Centre climate model: HadAM3. Clim. Dyn. 16, 123–146. https://doi.org/10.1007/s003820050009.

Renssen, H., Seppä, H., Heiri, O., Roche, D.M., Goosse, H., Fichefet, T., 2009. The spatial and temporal complexity of the Holocene thermal maximum. Nat. Geosci. 2, 411–414. https://doi.org/10.1038/ngeo513.

Sachs, J.P., Blois, J.L., McGee, T., Wolhowe, M., Haberle, S., Clark, G., Atahan, P., 2018. Southward shift of the Pacific ITCZ during the Holocene. Paleoceanogr. Paleoclimatol. 33, 1383–1395. https://doi.org/10.1029/2018PA003469.

Schilt, A., Baumgartner, M., Schwander, J., Buiron, D., Capron, E., Chappellaz, J., Loulergue, L., Schüpbach, S., Spahni, R., Fischer, H., Stocker, T.F., 2010. Atmospheric nitrous oxide during the last 140,000years. Earth Planet. Sci. Lett. 300, 33–43. https://doi.org/10.1016/j.epsl.2010.09.027.

Singarayer, J.S., Valdes, P.J., Roberts, W.H.G., 2017. Ocean dominated expansion and contraction of the late Quaternary tropical rainbelt. Sci. Rep. 7, 9382. https://doi.org/10.1038/s41598-017-09816-8.

Smith, R.S., Gregory, J.M., Osprey, A., 2008. A description of the FAMOUS (version XDBUA) climate model and control run. Geosci. Model Dev. 16.

Sundaram, S., Yin, Q.Z., Berger, A., Muri, H., 2012. Impact of ice sheet induced North Atlantic oscillation on East Asian summer monsoon during an interglacial 500,000 years ago. Clim. Dyn. 39, 1093–1105. https://doi.org/10.1007/s00382-011-1213-z.

Sundqvist, H.S., Kaufman, D.S., McKay, N.P., Balascio, N.L., Briner, J.P., Cwynar, L.C., Sejrup, H.P., Seppä, H., Subetto, D.A., Andrews, J.T., Axford, Y., Bakke, J., Birks, H.J.B., Brooks, S.J., de Vernal, A., Jennings, A.E., Ljungqvist, F.C., Rühland, K.M., Saenger, C., Smol, J.P., Viau, A.E., 2014. Arctic Holocene proxy climate database – new approaches to assessing geochronological accuracy and encoding climate variables. Clim. Past 10, 1605–1631. https://doi.org/10.5194/cp-10-1605-2014.

Tao, W., Huijun, W., Dabang, J., 2010. Mid-Holocene East Asian summer climate as simulated by the PMIP2 models. Palaeogeogr. Palaeoclimatol. Palaeoecol. 288, 93–102. https://doi.org/10.1016/j.palaeo.2010.01.034.

Thomas, E.R., Wolff, E.W., Mulvaney, R., Steffensen, J.P., Johnsen, S.J., Arrowsmith, C., White, J.W.C., Vaughn, B., Popp, T., 2007. The 8.2ka event from Greenland ice cores. Quat. Sci. Rev. 26, 70–81. https://doi.org/10.1016/j.quascirev.2006.07.017.

Wang, B., Fan, Z., 1999. Choice of south Asian summer. Bull. Am. Meteorol. Soc. 80, 10.

Wang, B., Wu, Z., Li, J., Liu, J., Chang, C.-P., Ding, Y., Wu, G., 2008a. How to measure the strength of the east Asian summer monsoon. J. Clim. 21, 4449–4463. https://doi.org/10.1175/2008JCLI2183.1.

Wang, N., Jiang, D., Lang, X., 2018. Northern westerlies during the last glacial maximum: results from CMIP5 simulations. J. Clim. 31, 1135–1153. https://doi.org/10.1175/JCLI-D-17-0314.1.

Wang, Y., Cheng, H., Edwards, R.L., Kong, X., Shao, X., Chen, S., Wu, J., Jiang, X., Wang, X., An, Z., 2008b. Millennial- and orbital-scale changes in the East Asian monsoon over the past 224,000 years. Nature 451, 1090–1093. https://doi.org/10.1038/nature06692.

Xiao, D., Zhao, P., Wang, Y., Zhou, X., 2016. Responses of the summer Asian-Pacific zonal thermal contrast and the associated evolution of atmospheric circulation to transient orbital changes during the Holocene. Sci. Rep. 6 https://doi.org/10.1038/srep35816.

Yin, Berger, A., Driesschaert, E., Goosse, H., Loutre, M.F., Crucifix, M., 2008. The Eurasian ice sheet reinforces the East Asian summer monsoon during the interglacial 500 000 years ago. Clim. Past 4, 79–90. https://doi.org/10.5194/cp-4-79-2008.

Yin, Q.Z., Berger, A., Crucifix, M., 2009. Individual and combined effects of ice sheets and precession on MIS-13 climate. Clim. Past 5, 229–243.

Yu, Z., Beilman, D.W., Jones, M.C., 2013. Sensitivity of northern peatland carbon dynamics to Holocene climate change. In: Baird, A.J., Belyea, L.R., Comas, X., Reeve, A.S., Slater, L.D. (Eds.), Geophysical Monograph Series. American Geophysical Union, Washington, D. C., pp. 55–69

Zhang, D., Feng, Z., 2018. Holocene climate variations in the Altai Mountains and the surrounding areas: a synthesis of pollen records. Earth Sci. Rev. 185, 847–869. https://doi.org/10.1016/j.earscirev.2018.08.007.

Zhang, J., Chen, F., Holmes, J.A., Li, H., Guo, X., Wang, J., Li, S., Lü, Y., Zhao, Y., Qiang, M., 2011. Holocene monsoon climate documented by oxygen and carbon isotopes from lake sediments and peat bogs in China: a review and synthesis. Quat. Sci. Rev. 30, 1973–1987. https://doi.org/10.1016/j.quascirev.2011.04.023.

Zhang, Y., Renssen, H., Seppä, H., 2016. Effects of melting ice sheets and orbital forcing on the early Holocene warming in the extratropical Northern

Hemisphere. Clim. Past 12, 1119–1135. https://doi.org/10.5194/cp-12-1119-2016.

Zhang, Y., Renssen, H., Seppä, H., Valdes, P.J., 2018. Holocene temperature trends in the extratropical Northern Hemisphere based on inter-model comparisons. J. Quat. Sci. 33, 464–476. https://doi.org/10.1002/jqs.3027.

Zhao, P., Zhu, Y., Zhang, R., 2007. An Asian–Pacific teleconnection in summer tropospheric temperature and associated Asian climate variability. Clim. Dyn.

29, 293–303. https://doi.org/10.1007/s00382-007-0236-y.

Zhang, X., Jin, L., Chen, J., Chen, F., Park, W., Schneider, B., Latif, M., 2017. Detecting the relationship between moisture changes in arid central Asia and East Asia during the Holocene by model-proxy comparison. Quat. Sci. Rev. 176, 36–50. https://doi.org/10.1016/j.quascirev.2017.09.012.